PHYSICAL REVIEW A VOLUME 17, NUMBER 3 MARCH 1978

Dissociative recombination in argon: Dependence of the total rate coefficient and excited-state production on electron temperature

Yueh-Jaw Shiu and Manfred A. Biondi

Department of Physics and Astronomy, University of Pittsburgh, Pittsburgh, Pennsylvania 15260

(Received 21 November 1977)

A three-mode microwave afterglow apparatus and high-speed grating spectrometer are used to study dissociative recombination in argon. The total rate coefficient may be represented by $\alpha[Ar_2^+] = 9.1 \times 10^{-7} \times [300/T_e(K)]^{0.61}$ cm^3/sec over the electron-temperature range $300 \leq T_e \leq 8500$ K, with $T_+ = T_{gas} = 300$ K. The excited states produced by the dissociative recombination are determined at $T_e = 300$ and 7200 K. In both cases, the $4p$ and $4p'$ states are found to be the most strongly populated.

I. INTRODUCTION

The present study of the dissociative recombination of Ar_2^+ ions with electrons,

$$Ar_2^+ + e^- \rightleftharpoons (Ar_2^*)_{repulsive} \to Ar^* + Ar\,, \qquad (1)$$

is a continuation of our investigation of electron capture by the diatomic molecular ions of the noble gases[1-3] using microwave afterglow techniques. The electron-temperature dependence of the total rate coefficient $\alpha(Ar_2^+)$ is redetermined[4] over the range $300 \leq T_e \leq 8500$ K, and the results are compared with other studies[4-7] of recombination in argon. Excited states originating from the dissociative recombination process are determined at $T_e = 300$ and 7200 K.

II. METHOD OF MEASUREMENT AND ANALYSIS

The microwave cavity/waveguide afterglow apparatus and grating spectrometer used in this study have been described in detail previously.[3] The argon used in the studies is research grade from the Linde Division of Union Carbide Corp. A microwave discharge pulse lasting 1.5 msec and repeated at a 60-Hz rate is employed for plasma generation. The electron density decay during the afterglow is determined from measurements of the shift in resonant frequency of the cavity mode. At the microwave frequency ($\omega = 1.93 \times 10^{10}$ Hz) and argon pressures (typically 5 to 15 Torr) used in this study the correction of the frequency-shift data for finite collision frequency effects is negligible (<1%) for the electron temperatures of interest.

Computer solutions of the electron continuity equation,

$$\frac{\partial n_e(\vec{r}, t)}{\partial t} \simeq -\alpha n_e^2 + D_a \nabla^2 n_e\,, \qquad (2)$$

are compared with the measured electron density decays to determine α, the recombination rate coefficient. Known values of the ambipolar diffusion coefficient $D_a = D_+(1 + T_e/T_+)$, obtained from the measured mobility[8] of Ar_2^+ in Ar, are used in the continuity equation.

The afterglow line emission radiation has been determined by means of a grating spectrometer and photomultiplier detector. The spectral response of the overall system over the range $3800 < \lambda < 8900$ Å has been determined by calibration against a tungsten "grey-body" source operated at 2850 K.

III. RESULTS

Examples of several of the fits of the solutions of Eq. (2) to the experimental data at $p = 10$ Torr are given in Fig. 1. The data are plotted in the form $1/\bar{n}_{\mu w}$ vs t, where $\bar{n}_{\mu w}$ is the microwave-averaged electron density. Over the pressure range 5 to 15 Torr, we find no systematic variation (<5%) in the inferred α values at $T_e = T_+ = T_n = 300$ K. The values of $\alpha(Ar_2^+)$ derived from data such as shown in Fig. 1 are given in Fig. 2. The variation of the total rate coefficient with electron temperature can be represented, within ±10%, by

$$\alpha(\text{cm}^3/\text{sec}) = 9.1 \times 10^{-7}[300/T_e(\text{K})]^{0.61}. \qquad (3)$$

The $\alpha(T_e)$ values obtained at argon pressures of 7 and 10 Torr agree within 10% over the temperature range $300 \leq T_e \leq 8500$ K.

The excited states produced by two-body, dissociative recombination of electrons and Ar_2^+ ions are identified by the fact that the emission intensity from such states varies as n_e^2. Examples of the relative variation of $I^{1/2}$ and n_e for some typical transitions are given for $T_e = T_n = T_+ = 300$ K in Fig. 3 and for the heated case $T_e = 7200$ K in Fig. 4. In both cases, excellent tracking between $I^{1/2}$ and $\bar{n}_{\mu w}$ is observed. Within our detection range, $\sim 3800 < \lambda < \sim 8900$ Å, a total of 19 transitions which exhibit a recombination origin were identified for the unheated case ($T_e = 300$ K) and

© 1978 The American Physical Society

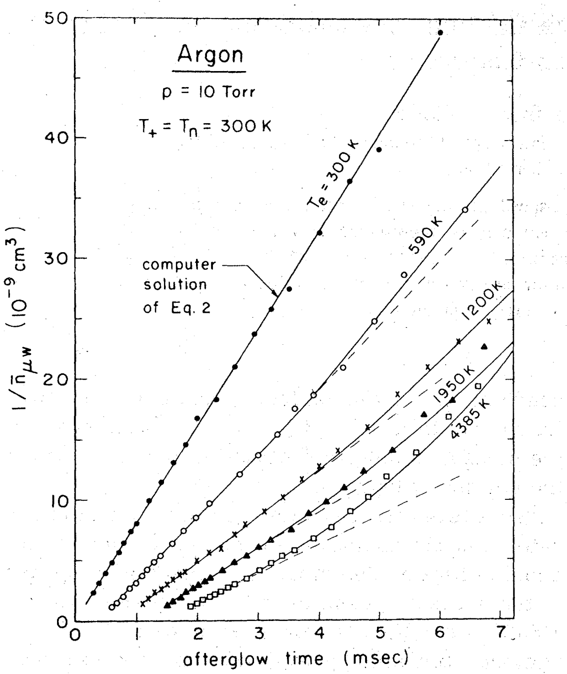

FIG. 1. Reciprocal of the "microwave-averaged" electron density vs time, with electron temperature as a parameter. The zero afterglow times of successive curves are displaced 0.4 msec for clarity. The solid lines are fits to the data of computer solutions of Eq. (2).

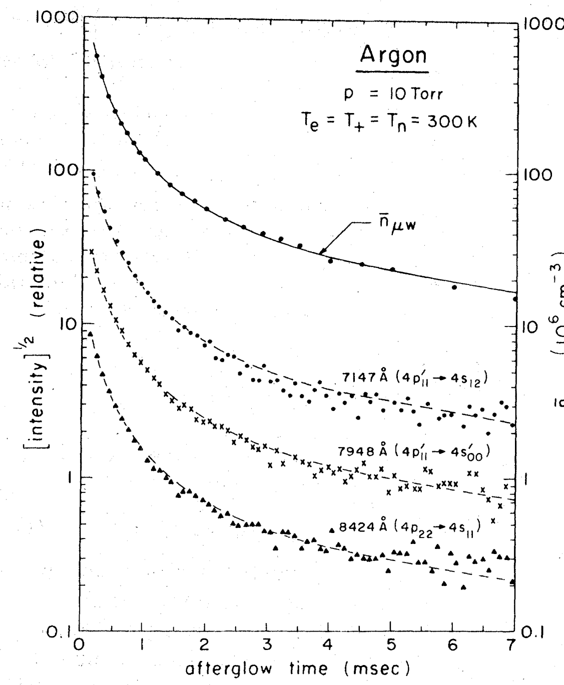

FIG. 3. Comparison of the variation of electron density $\bar{n}_{\mu w}$ and the square root of the afterglow intensity $I^{1/2}$ for representative transitions for the case $T_e = T_+ = T_n = 300$ K. The dashed lines through the $I^{1/2}$ data represent renormalized $\bar{n}_{\mu w}$ data. Modified Racah notation is used to designate the states.

are listed in Table I, together with their relative intensities. Twenty additional transitions resulting from recombination into higher-lying states were observed during heating to $T_e = 7200$ K; these are also listed in Table I. The relative intensities are determined by gating the photon-counting cir-

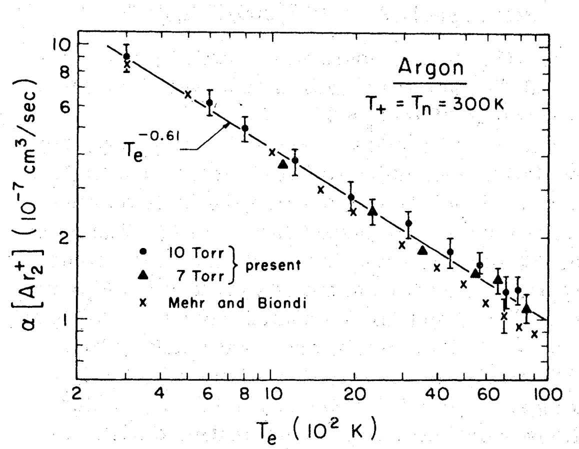

FIG. 2. Measured variation of $\alpha(Ar_2^+)$ with electron temperature for $T_+ = T_n = 300$ K. The solid line represents a simple power-law variation as $T_e^{-0.61}$.

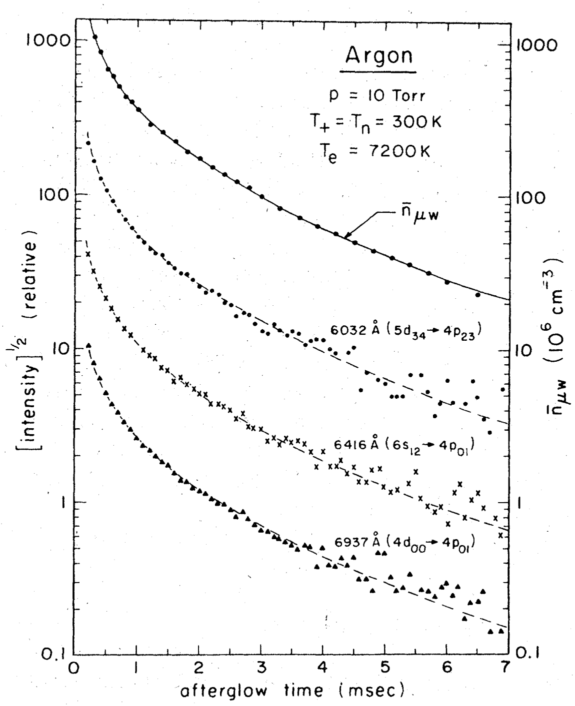

FIG. 4. Comparison of the variation of $\bar{n}_{\mu w}$ and $I^{1/2}$ during the afterglow for some of the higher-lying transitions observed during heating to $T_e = 7200$ K.

TABLE I. Transitions originating from dissociative recombination of Ar_2^+ ions and electrons and their relative intensities in unheated (T_e = 300 K) and heated (T_e = 7200 K) afterglows. Modified Racah notation is used to designate the states.

Wavelength (Å)	Upper state	Lower state	Intensity (T_e = 300 K)	Intensity (T_e = 7200 K)
4158	$5p_{12}$	$4s_{12}$	...	13
4164	$5p_{11}$	$4s_{12}$	...	2
4181	$5p'_{01}$	$4s'_{00}$	...	1
4190	$5p_{22}$	$4s_{12}$ }	...	3
4191	$5p'_{11}$	$4s'_{00}$ }		
4198	$5p_{00}$	$4s_{11}$	...	2
4200	$5p_{23}$	$4s_{12}$	...	10
4266	$5p_{12}$	$4s_{11}$	...	1
4272	$5p_{11}$	$4s_{11}$	...	3
4300	$5p_{00}$	$4s_{11}$	...	5
4333	$5p'_{12}$	$4s'_{01}$	...	2
4335	$5p'_{01}$	$4s'_{01}$	...	1
6032	$5d_{34}$	$4p_{23}$	...	2
6043	$5d_{33}$	$4p_{22}$	...	1
6416	$6s_{12}$	$4p_{01}$	...	2
6677	$4p'_{00}$	$4p_{01}$	2	5
6752	$4d_{12}$	$4p_{01}$	...	8
6871	$4d_{01}$	$4p_{01}$	...	7
6937	$4d_{00}$	$4p_{01}$	...	2
6965	$4p'_{01}$	$4s_{12}$	80	120
7030	$6s_{12}$	$4p_{23}$	...	5
7067	$4p'_{12}$	$4s_{12}$	50	70
7147	$4p'_{11}$	$4s_{12}$	13	20
7272	$4p'_{01}$	$4s_{11}$	40	60
7353	$4d_{33}$	$4p_{22}$	...	2
7372	$4d_{34}$	$4p_{23}$	...	8
7383	$4p'_{12}$	$4s_{11}$	80	130
7503	$4p'_{00}$	$4s'_{01}$	130	200
7514	$4p_{00}$	$4s_{11}$	90	150
7635	$4p_{12}$	$4s_{12}$	200	330
7723	$4p_{11}$	$4s_{12}$	160	260
7948	$4p'_{11}$	$4s'_{00}$	150	240
8006	$4p_{12}$	$4s_{11}$	95	180
8014	$4p_{22}$	$4s_{12}$	140	220
8103	$4p_{11}$	$4s_{11}$	210	320
8115	$4p_{23}$	$4s_{12}$	340	560
8264	$4p'_{01}$	$4s'_{01}$	300	440
8408	$4p'_{12}$	$4s'_{01}$	410	740
8424	$4p_{22}$	$4s_{11}$	450	720
8521	$4p'_{11}$	$4s'_{01}$	240	390

cuitry on during the interval 0.2–15 msec in the afterglow.

IV. DISCUSSION AND CONCLUSIONS

A. Total rate coefficient

The present study yields a value $\alpha(Ar_2^+) = (9.1 \pm 0.9) \times 10^{-7}$ cm^3/sec at 300 K, which is in excellent agreement with the measurement of Mehr and Biondi[4] (using essentially the same apparatus) and in reasonable agreement with Biondi[5] and with Oskam and Mittelstadt.[6]

The electron temperature dependence, $\alpha(Ar_2^+) \sim T_e^{-0.61}$, measured over the range $300 \leq T_e \leq 8500$ K, agrees within the ±10% experimental uncertainty with Mehr and Biondi's result,[4] $\alpha(Ar_2^+) \sim T_e^{-0.67}$. The difference between our result and Fox and Hobson's $\sim T_e^{-1.3}$ variation[7] (obtained in shock-heated argon) has been explained by Mehr and Biondi[4] on the basis that shock heating leads to some excitation of the Ar_2^+ from their ground vibrational state ($v = 0$) to excited vibrational states ($v \geq 1$) which are expected to exhibit smaller recombination coefficients because of less favorable overlap between the initial and intermediate states indicated in reaction (1).

B. Excited states produced by recombination

The excited states formed by the dissociative recombination process in argon are similar in some respects to those observed in xenon[1] and krypton[2], as may be seen from the representative transitions shown on the partial energy-level diagram of argon (Fig. 5). As with xenon and krypton at $T_e = 300$ K, no states are produced which lie above the ground electronic and vibrational state of the Ar_2^+ ions. Unfortunately, transitions from the $3d$, $3d'$, $5s$, and $5s'$ groups of states, which lie below but within ~0.5 eV of the Ar_2^+ ($v = 0$) level, fall outside the wavelength-detection range of our apparatus. We do not observe transitions from levels of the $5p$ group, even though they are within our detection range. This suggests that the binding energy of Ar_2^+ may lie closer to Mulliken's theoretical value[9] of 1.4 eV, labeled *T* in Fig. 5, than to the experimentally deduced value[10] of 1.23 ± 0.02 eV, labeled *E*. [As this paper was being readied for publication we learned of a new determination[11] of the Ar_2^+ binding energy by photofragment spectroscopy techniques. The value obtained, 1.33 ± 0.02 eV, fits our spectroscopic observations quite well.]

With electron heating to $T_e \sim 7200$ K (mean electron energy ~0.8 eV), additional states, lying as much as 0.6–0.8 eV above the Ar_2^+ ($v = 0$) state, are observed. Here, as with krypton and xenon, we do not observe transitions emanating from all energetically allowed states; in the present case transitions from $5d$ but not from the lower-lying $6s'$ and $4d'$ states are observed (the $6p$ transitions are outside our detection range); in krypton population of the $6d$ but not the lower-lying

TABLE II. Transitions originating from dissociative recombination of Xe_2^+ ions and electrons and their relative intensities in unheated ($T_e = 300$ K) and heated ($T_e = 7500$ K) afterglows. Modified Racah notation is used to designate the states.

Wavelength (Å)	Upper state	Lower state	Intensity ($T_e = 300$ K)	Intensity ($T_e = 7500$ K)
4501	$6p'_{01}$	$6s_{12}$	6	4
4525	$6p'_{12}$	$6s_{12}$	4	2
4583	$6p'_{00}$	$6s_{11}$	2	1
4624	$7p_{12}$	$6s_{12}$	13	9
4671	$7p_{23}$	$6s_{12}$	21	17
4697	$7p_{22}$	$6s_{12}$	4	1
4734	$6p'_{12}$	$6s_{11}$	5	5
4807	$7p_{00}$	$6s_{11}$	5	4
4830	$7p_{11}$	$6s_{11}$	5	2
4843	$7p_{12}$	$6s_{11}$	5	4
4917	$6p'_{11}$	$6s_{11}$	4	3
4923	$7p_{22}$	$6s_{11}$	5	3
6318	$8d_{34}$	$6p_{23}$	···	4
6504	$8p_{00}$	$6s_{01}$	···	3
6543	$9s_{12}$	$6p_{22}$	···	1
6827	$4f_{11}$	$6s'_{00}$	···	4
6872	$6f_{45}$	$5d_{34}$	···	6
6882	$7d_{33}$	$6p_{22}$	···	9
7120	$7d_{34}$	$6p_{23}$	···	16
7336	$5d'_{23}$	$6p_{22}$	···	2
7394	$7d_{23}$	$6p_{12}$	···	9
7584	$5f_{45}$	$5d_{34}$	···	18
7642	$6p'_{01}$	$6s'_{00}$	30	60
7802	$8s_{11}$	$6p_{22}$	···	8
7887	$6p'_{00}$	$6s'_{01}$	15	26
7967	$7p_{11}$	$6s'_{00}$	19	32
8206	$6p'_{11}$	$6s'_{00}$	27	50
8232	$6p_{12}$	$6s_{12}$	360	600
8267	$6p'_{01}$	$6s'_{01}$	23	44
8280	$6p_{00}$	$6s_{11}$	400	750
8347	$6p'_{12}$	$6s'_{01}$	80	180
8409	$6p_{11}$	$6s_{12}$	25	70
8819	$6p_{23}$	$6s_{12}$	$\gtrsim 1000$	$\gtrsim 1000$

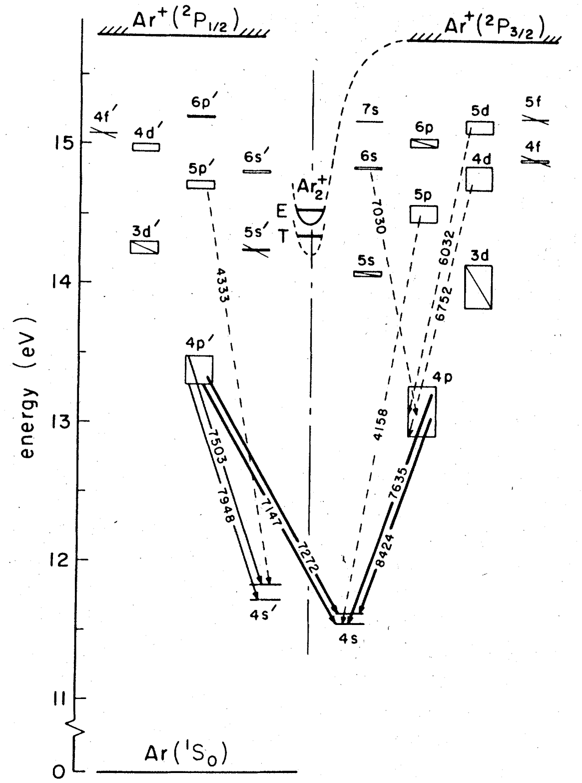

FIG. 5. Partial energy-level diagram for argon showing representative transitions observed to result from dissociative recombination of Ar_2^+ ions with electrons. The weights of the lines indicate qualitatively the radiation intensity; solid lines, $T_e = T_n = 300$ K; dashed lines, additional transitions observed at $T_e = 7200$ K. A diagonal line through a state indicates that transitions from that state fall outside our wavelength detection range. The positions of the ground state of Ar_2^+ labeled T and E are from theoretical calculation (Ref. 9) and experiment (Ref. 10), respectively.

$7p$ states was observed, and in xenon the $8d$ but not the $9p$ was observed.

In both the unheated and heated cases, the $4p$ and $4p'$ states are the most strongly populated, a finding in keeping with the results for krypton, where transitions from the $5p$ and $5p'$ states have the highest intensities and for xenon, where transitions from the $6p$ states are the most intense. (The xenon transitions, which were merely ranked in order of decreasing intensity in the original paper,[1] have been reexamined. The relative intensities for both the unheated and heated cases are given in Table II.) We find that in argon, as in krypton and in xenon, dissociative recombination leads to formation of excited states belonging to both the $^2P_{3/2}$ and $^2P_{1/2}$ ion cores and that, in the unheated case ($T_e = 300$ K), essentially all energetically allowed (and detectable) transitions are observed. In the heated case ($T_e \simeq 7000$ K) the absence or weakness of certain transitions emanating from excited states lying above the molecular ion ground state may reflect competition between radiative decay and associative ionization of the state via the reaction $R^* + R \rightarrow R_2^+ + e^-$, where R indicates a rare-gas atom. For example, at the typical rare-gas pressures (~10 Torr) used in our studies, the possibility of a large rate coefficient ($\geq 10^{-9}$ cm^3/sec) for associative ionization[12] means that the lifetime against nonradiative loss of such an excited state may be substantially less than 10^{-8} sec.

ACKNOWLEDGMENTS

The authors wish to thank V. Jog for assistance with the data taking. This research was supported, in part, by the Advanced Research Projects Agency of the Department of Defense and was monitored by ONR under Contract No. N00014-76-C-0098.

APPENDIX

The relative intensities of transitions associated with dissociative recombination in xenon[1] have been determined for the period 0.5–10 msec during the afterglow and are given in Table II.

[1] Y. J. Shiu, M. A. Biondi, and D. P. Sipler, Phys. Rev. A 15, 494 (1977).

[2] Y. J. Shiu and M. A. Biondi, Phys. Rev. A 16, 1817 (1977).

[3] L. Frommhold, M. A. Biondi, and F. J. Mehr, Phys. Rev. 165, 44 (1968).

[4] F. J. Mehr and M. A. Biondi, Phys. Rev. 176, 322 (1968).

[5] M. A. Biondi, Phys. Rev. 129, 1181 (1963).

[6] H. J. Oskam and V. R. Mittelstadt, Phys. Rev. 132, 1445 (1963).

[7] J. N. Fox and R. M. Hobson, Phys. Rev. Lett. 17, 161 (1966).

[8] See, for example, E. W. McDaniel and E. A. Mason, *The Mobility and Diffusion of Ions in Gases* (Wiley, New York, 1973).

[9] R. S. Mulliken, J. Chem. Phys. 52, 5170 (1970).

[10] C. Y. Ng, D. J. Trevor, B. H. Mahan, and Y. T. Lee, J. Chem. Phys. 66, 446 (1977).

[11] J. T. Moseley, R. P. Saxon, B. A. Huber, P. C. Cosby, R. Abouaf, and M. Tadjeddine, J. Chem. Phys. 67, 1659 (1977).

[12] P. M. Becker and F. W. Lampe, J. Chem. Phys. 42, 3857 (1965).